Title

SuFExable polymers with helical structures derived from thionyl tetrafluoride

Journal

Nature Chemistry, 13(9)

ISSN

1755-4330

Authors

Li, Suhua

Li, Gencheng

Gao, Bing

et al.

Publication Date

2021-09-01

DOI

10.1038/s41557-021-00726-x

Peer reviewed

HHS Public Access

Author manuscript

Nat Chem. Author manuscript; available in PMC 2022 September 01.

Published in final edited form as:

Nat Chem. 2021 September ; 13(9): 858–867. doi:10.1038/s41557-021-00726-x.

SuFExable Polymers with Helical Structures Derived from Thionyl Tetrafluoride

Suhua Li[1,2,*], **Gencheng Li**[2], **Bing Gao**[2], **Sidharam P. Pujari**[3], **Xiaoyan Chen**[1], **Hyunseok Kim**[2], **Feng Zhou**[4], **Liana M. Klivansky**[5], **Yi Liu**[5], **Hafedh Driss**[6], **Dong-Dong Liang**[3], **Jianmei Lu**[4], **Peng Wu**[7,*], **Han Zuilhof**[3,6,8,*], **John Moses**[9,*], **K. Barry Sharpless**[2,*]

[1]School of Chemistry, Sun Yat-Sen University, 135 Xingang Xi Road, Guangzhou 510275, People's Republic of China

[2]Department of Chemistry and The Skaggs Institute for Chemical Biology, The Scripps Research Institute, 10550 North Torrey Pines Road, La Jolla, CA 92037, USA

[3]Laboratory of Organic Chemistry, Wageningen University, Stippeneng 4, 6708 WE Wageningen, The Netherlands

[4]College of Chemistry, Chemical Engineering and Materials Science, Collaborative Innovation Center of Suzhou, Nano Science and Technology, Soochow University, Suzhou 215123, China.

[5]The Molecular Foundry, Lawrence Berkeley National Laboratory, Berkeley, California 94720, USA.

[6]Department of Chemical and Materials Engineering, Faculty of Engineering, King Abdulaziz University, Jeddah, Saudi Arabia.

[7]Department of Molecular Medicine, The Scripps Research Institute, La Jolla, California 92037, USA.

[8]School of Pharmaceutical Sciences and Technology, Tianjin University, 92 Weijin Road, Tianjin, People's Republic of China.

[9]Cold Spring Harbor Laboratory, 1 Bungtown Road, New York, NY 11724, USA.

Abstract

Sulfur(VI) fluoride exchange (SuFEx) is a category of click chemistry that enables covalent linking of modular units through sulfur(VI) connective hubs. The efficiency of SuFEx and the stability of the resulting bonds have led to polymer chemistry applications. Now, we report the

* sharples@scripps.edu; moses@cshl.edu; han.zuilhof@wur.nl; pengwu@scripps.edu; lisuhua5@mail.sysu.edu.cn.

Author contributions

K. B. S., J. E. M., and H. Z. supervised the work. S. L., K. B. S., P. W., J. L., and J. E. M. conceived and designed the syntheses of the SOF_4-derived polymers. S. L., G. L., B. G., S. P. P., X. C., and H. K. performed the synthesis and characterization of the polymers. F. Z., L. M. K., Y. L., and J. Lu collected and analyzed the DSC and TGA data of all polymers. F. Z. collected the XRD data. S. P. P. performed molecular modeling, AFM, and scanning Auger experiments. H. D. performed the SEM and TEM experiments. D. L. collected the CD data. S. L., H. Z., K. B. S, and J. E. M. contributed to the preparation of the manuscript. All authors discussed the results and commented on the manuscript.

Competing interests

The authors declare the following competing financial interest(s): Sharpless, K. B., Wu, P.; Li, S.; Liu, Z.; Gao, B., patent applicant: The Scripps Research Institute, Thionyl tetrafluoride modified compounds and uses; provisional patent application Serial Number US62/427,489, filed on Nov/29/2016. International patent application no. PCT/US2017/063746. Status: Pending.

SuFEx click chemistry synthesis of several structurally diverse SOF_4-derived copolymers based upon the polymerization of bis(iminosulfur oxydifluorides) and bis(aryl silyl ethers). This polymer class presents two key characteristics: First, the [-N=S(=O)F-O-] polymer backbone linkages are themselves SuFExable and undergo precise SuFEx-based post-modification with phenols or amines to yield branched functional polymers. Second, studies of individual polymer chains of several of these new materials indicate helical polymer structures. The robust nature of SuFEx click chemistry offers the potential for post-polymerization modification, enabling the synthesis of materials with control over composition and conformation.

The inspiration behind modular click chemistry's invention came from an appreciation of how Nature synthesizes its most essential molecules, the primary metabolites. These polynucleotides, polypeptides, and polysaccharides from the union of discrete modules by carbon-heteroatom connections [1,2]. Since describing the underpinning philosophy of click chemistry, two key click reactions have emerged that enable the formation of stable connections with unparalleled efficiency. The Cu(I)-catalyzed azide-alkyne cycloaddition reaction (CuAAC) was reported independently by the groups of Meldal[3] and Shrapless[4] in 2002, whereas Sharpless and co-workers advanced the Sulfur Fluoride Exchange (SuFEx) reaction in 2014[5]. CuAAC has had a perspective-changing impact in many fields; not least, drug discovery[6–9], bioconjugation[10,11], and materials science[12–15]. In polymer chemistry, CuAAC is predominately used for backbone functionalization rather than for polymerization[16,17].

SuFEx click chemistry[18–22] is characterized by the exchange of aryl silyl ethers or amines, often through discrete SuFExable hubs such as sulfuryl fluoride (**SO_2F_2**)[5], thionyl tetrafluoride (**SOF_4**)[23,24], ethenesulfonyl fluoride (**ESF**)[5,18,25] and 1-bromoethene-sulfonyl fluoride (**BESF**)[26–28] (Figure 1). Dong, Gao, and co-workers were among the first to recognize the potential of SuFEx for polymer synthesis. Exploiting the powerful combination of reaction efficiency and linkage stability, the researchers synthesized several SO_2F_2-derived polysulfate-SuFEx copolymers of bis(aryl silyl ethers) with bis(aryl fluorosulfates) in the presence of 1,8-diazabicyclo[5.4.0]undec-7-ene (DBU) or highly efficient catalyst $(Me_2N)_3S^+[FHF]^-$ (Figure 1b) [29,30]. Wu and co-workers reported the high yielding synthesis of polysulfonate SuFEx polymers, employing a bifluoride ion-catalyzed polycondensation of ESF-derived bis(alkylsulfonyl fluorides) with bis(aryl silyl ethers) (Figure 1b)[31]. The mild conditions enable SuFEx polymerization reactions to proceed efficiently without causing significant increases in temperature during the reaction[29,30], delivering novel materials with fascinating properties, including hydrolytic stability, thermal stability, and tensile modulus.

Encouraged by the successful applications of SO_2F_2 and ESF in SuFEx polymer chemistry, we have explored thionyl tetrafluoride (SOF_4) as a new connective hub[23] for use in polymer synthesis. Unlike the SO_2F_2 and ESF SuFExable hubs, SOF_4 is a multidimensional connector that forms discrete connections via a stereogenic sulfur(VI) center [e.g., R–N=**S**(=O)(F)–OR'].

The unique connectivity potential of SOF_4 creates countless opportunities for click chemistry[23], and in the context of polymer science, a chance to overcome the incredibly challenging goal of post-polymerization modification of the polymer spine (Figure 1c).

Herein, we report the synthesis of an unprecedented family of helical SuFEx polymers from copolymerization of bis(aryl silyl ethers) and the SOF_4 derived bis(iminosulfur oxydifluorides).

The powerful combination of highly efficient SuFEx-reactivity and robust SuFEx-enabled post-polymerization modifications enables the synthesis of materials with rational control of composition, conformation, and functionality.

Results and Discussion

Polymer synthesis.

The bis(iminosulfur oxydifluoride) (**1–1**) (prepared as previously described from SOF_4[23] and 4,4'-diaminodiphenyl sulfone), and the bisphenol A bis(*t*-butyldimethylsilyl ether)[29,30] (**2–1**) were chosen as model substrates. In our earlier SuFEx work with SOF_4, we found that under DBU catalysis, it is possible to exchange just one of the bis(iminosulfur oxydifluoride) S–F bonds. The products comprise a single S–F bond, which is significantly less reactive due to the attenuated electrophilicity as sulfur; nevertheless, under more forcing SuFEx conditions, this S–F bond is also exchangeable. We anticipated that using sub-stoichiometric quantities of DBU would allow the polymerization process to proceed through just one of the two available S–F bonds of each iminosulfur oxydifluoride group, thereby avoiding cross-linking and branching reactions[23].

The addition of DBU (2 mol %)[5,29], to a solution of the difluoride (1 equiv), and silyl ether (1 equiv) in *N*-methyl-2-pyrrolidone (NMP) at room temperature gave an observable reaction almost immediately, with the solution becoming noticeably more viscous. Stirring the reaction mixture for a further 5 min resulted in forming a syrupy solution accompanied by a slight increase in the reaction temperature (to 40 ~ 50 °C). After 3.5 h reaction time, the colorless [Ar–N=S(=O)(F)–OAr]-linked polymer **3–1** was isolated in 99% yield with an Mw of 197 kDa, (i.e., containing ca. 326 monomers, and a polydispersity index (PDI) of 1.8) (Figure 1d)[32].

With confirmation that the SOF_4 derived iminosulfur oxydifluoride connectors are incorporated smoothly into the polymer spine, we next explored the potential of this SuFEx-polymerization reaction to access structurally different polymers from a diverse set of building blocks. Hence, the DBU mediated polymerization of **1–1** was examined with aryl silyl ethers comprising different functional groups (**2–1** ~ **2–12**), giving the respective polymers **3–1** ~ **3–12** in excellent yields (82 to 99%, Table 1), with the distribution of molecular weights ranging from 36 to 295 kDa and typical PDIs of ~1.7 (values ranging from 1.4 to 2.3). Similarly, the SuFEx polymerization reaction worked equally well with a selection of bis(iminosulfur oxydifluorides) (themselves prepared from SOF_4 and the corresponding bis-arylamines) and several bis(aryl silyl ethers) delivering various polymers (**3–13** to **3–31**) with excellent yields. Due to the lower reactivity of benzylic substrates, both

the *meta* and *para*-bis(benzylic iminosulfur oxydifluorides) required more extended reaction times (24 h) and an increased catalyst loading of 10 mol% DBU (**3–32**, **3–33**).

Examining the collective ^{1}H NMR, ^{13}C NMR, and ^{19}F NMR data of the polymers revealed surprisingly uncomplicated spectra as if belonging to a small molecule [See Supplementary page 98 ~ 145]. Considering that the connective sulfur center is stereogenic and could result in numerous diastereoisomers in an uncontrolled polymerization event, the spectra are curiously straightforward.

To investigate the polymerization progress in more detail, the DBU catalyzed copolymerization of **1–1** and **2–1** was monitored by sampling and quenching 20 μL aliquots of the reaction mixture every 10 seconds. The transformation data was calculated based on the ratio of ^{19}F signal integral of the remaining -N=SOF_2 to the initial -N=SOF_2 before adding DBU. The NMR data (see Supplementary page 161 ~ 171) revealed that the monomer conversion was completed within 200 seconds (Figure 2). The relative ratios of the ^{19}F signals at 48.4 ppm and 48.2 ppm in the NMR spectra show a substantial initial increase of the terminal fluoride, followed by a gradual decrease as the polymerization ensues. These observations are characteristic of a step-growth polymerization mechanism[33].

Polymer functionalization.

Post-polymerization modification (PPM) is an important technique that allows the manipulation of polymer properties through synthetic modification and derivitization[34–38]. Hence, the SuFEx modification of the remaining S(VI)–F bond of the polymeric materials is advantageous. Studies on the chemistry of SOF_4 derivatives revealed that 2-*tert*-butylimino-2-diethylamino-1,3-dimethylperhydro-1,3,2-diazaphosphorine (BEMP) is an effective catalyst for the SuFEx of aryl silyl ethers with the remaining S(VI)–F bond of sulfurofluoridoimidates[23]. The same is true for the SOF_4 derived polymers; upon the reaction of polymer **3–1** with *tert*-butyldimethyl(4-(1,2,2-triphenylvinyl)phenoxy)silane (**4**) and BEMP (10 mol %), the backbone modified polymer **5** was isolated in 95% yield (Figure 3a). Unlike the precursor polymer **3–1**, the derivative **5** displays a strong aggregation-induced emission (AIE) effect[39], dramatically enhancing photoluminescence efficiency as water content increases from 0% to 99%. This observation is significant because AIE fluorophores have applications in many fields, including energy, optoelectronics, and life science, thereby presenting a significant opportunity for SOF_4-SuFEx polymers (Figure 3b) [For fluorescence spectra of polymer **3–1** and 4-(1,2,2-triphenylvinyl)phenol, see Supplementary pages 51–52.]

Additionally, the SuFEx derivatization of the polymer **3–1** with the *tert*-butyl(3-ethynylphenoxy) dimethylsilane (**6**) delivers the alkyne-functionalized polymer **7** in excellent yield (Figure 3c). The remarkable efficiency of the reaction is confirmed by the degree of substitution of at least 93% based on the ratio of methyl vs. terminal alkynyl protons in the ^{1}H NMR (see Supplementary page 147)[40]. The alkyne unit's surgical installation enables further click chemistry functionalization through CuAAC, thereby offering a unique modular platform for creating novel functional polymers. This feature was demonstrated through the further derivatization of the polymer **7** with the azidothymidine (AZT) **8** under ligand-accelerated CuAAC conditions[41,42] to give the triazole-linked

nucleoside polymer **9** in 96% yield. Analysis of the ^{1}H NMR spectrum revealed that, as far as observable from the absence of any remaining terminal alkyne protons, all pendant alkyne groups of the parent polymer had been consumed (see Supplementary page 148).

The reaction of the remaining S–F bonds of the SuFEx polymer **3–1** was also feasible with the secondary amines such as pyrrolidine (**10**) and 4-ethynylpiperidine (**11**), yielding the branched polymers **12** and **13** conveniently (Figure 3d), or with ferrocene moieties in **14** to yield polymer **15** (Figure 3E).

Polymer structure.

The uncomplicated ^{1}H NMR, ^{13}C NMR, and ^{19}F NMR spectra of all the new SuFEx polymers inspired us to explore further the 3D structure of these new materials. Because of the tetrahedral sulfur core of the ~N=**S**(=O)F–O~ linkage, we anticipated that the SOF_4-based polymers might also display three-dimensional features beyond random coiling, as observed for a variety of helical polymers[43,44]. We, therefore, assessed three representative SuFEx polymers: first **3–23**, and subsequently **3–9** and **5** by atomic force microscopy (AFM, tapping mode); molecular mechanics studies; scanning Auger microscopy; high-resolution scanning electron microscope (SEM); and transmission electron microscopy (TEM) measurements.

First, we built a 32-mer atomistic model of the polymer **3–23**, and the structure thereof was optimized with a generically applicable force field for organic materials (PCFF force field)[45] without any constraints. This model yielded a helical structure with a diameter of 4.9 ± 0.4 nm and a pitch of 7.0 nm (Figure 4a–b). Experimental studies of individual surface-deposited polymer chains followed.

Polymer **3–23** was dissolved in dichloromethane, and a few droplets of the solution dispensed onto an atomically flat, hexadecyne-coated Si(111) surface[46], after which the solvent was allowed to evaporate at room temperature. Next, AFM topography images of **3–23** were obtained as deposited on these Si(111) surfaces, which displayed many individual polymer wires (Figure 4c–g). These individual polymer chains revealed a near-constant height of 4.2 ± 0.7 nm (insert in Figure 4c measured at 370 points on multiple polymer chains, like those in Figure 4d, on the surface; see also Supplementary Figure 10). This height surpasses the size of any moiety present in the polymer chain of **3–23** but correlates very well to the theoretical prediction of a helix's diameter formed by individual polymer chains. More detailed information on the polymer structure can be obtained from Figure 4e, which depicts the corresponding amplitude signal map, revealing periodicity in the polymeric structures. To rule out effects of the substrate and scanning parameters on the observed periodicity, we compared the cross-sectional profiles of the polymer along the main axis of symmetry (vertical purple line in Fig. 4e), with a profile line along the same direction on the substrate (vertical yellow line in Fig. 4e). The amplitude cross-section on the polymer showed a clear periodic signal, which is not present on the substrate (Fig.4f). Fast Fourier Transform (FFT) on the cross-sectional profile of the polymer was used to evaluate the polymer periodicity quantitatively(Fig. 4g). The experiment revealed a dominant frequency of ca. 7 nm in agreement with the polymer's calculated structure.

As expected, a similar operation on the profile acquired on the substrate did not show any significant periodicity, thus excluding scanning artifacts or substrate influence.

To corroborate the polymer height obtained by AFM, we next performed high-resolution SEM analysis to determine the width of individual polymer chains, revealing a figure of 4.8 ± 0.5 nm (measured at 50 points on multiple polymer chains on the surface; Figure 4h). The height and width agree very well with one another and the hypothesized helical character of polymer wires (**3–23**). To confirm that the observed wires did indeed correspond to the SuFEx polymer, instead of some unidentified fibrous contamination, we performed scanning Auger microscopy (on a hexadecanethiol-modified Au surface). As can be seen in Figure 4i, the wire-like structures comprise the elements expected to be present in the polymer chain, namely O, C, S, N, and F; thus corroborating that indeed the SuFEx polymer wires with functional ~N=S(=O)F–O~ moiety were being observed. Finally, high-resolution TEM measurements allowed the zooming in on the structure. First, the TEM measurements (Figure 4k) at 30 points revealed a width of 4.5 ± 0.6 nm for individual polymer chains, in agreement with both SEM and modeling data, thereby strongly indicating a helical structure. Second, the zoomed-in TEM data in Figure 4j and 4l revealed a repeating structure. The red triangles in these figures are placed at points of increased intensity, which occur at highly regular intervals, as expected for a single helical polymer. This regularity is observable for individual polymer chains (Figure 4j) and chains adjacent to each other (Figure 4l). Analogous to the polymer-structure optimized *in vacuo* that yields a pitch of 7.0 nm and the AFM data that yields a pitch of ca. 7 nm, the high-resolution TEM image yields a polymer pitch of ca. 4.6 ± 0.6 nm (at 31 points). We tentatively attribute these differences to the attractive polymer-surface interactions and sample-to-sample variations. Such helical structures are consistent with the NMR data since random configurations would lead to broad NMR peaks, contrasting with observation.

Molecular modeling studies on 20 of the polymers from Figure 2 predict that all form helical structures, although, for most polymers, the helical structure only displays a diameter less than 1.5 nm, which would be hard to detect by AFM. We surmised that the size of the groups would strongly affect the diameter of the polymer chain. To this end, we investigated the structure of **5** (as a polymer with a bulky substituent) and **3–9** (as a representative polymer with relatively small groups) in detail. Indeed, both **3–9** and **5** displayed helical structures in the modeling, with diameters of 5.7 ± 0.4 nm and 2 ± 1 nm, respectively. These values correlate very well with AFM-measured heights of 6.9 ± 1.1 nm and 2.1 ± 0.2 nm, respectively, as well as the TEM-observed widths of 5.5 ± 0.3 nm and 2.3 ± 0.4 nm, respectively (see Supplementary Figure 16 and 13 on pages 65, 63). The latter is in the range observed for double-stranded DNA helices (2.3 ± 0.2 nm).[47] Finally, large substituents do not always yield high diameters. For example, the ferrocene-linked polymer **15** was synthesized to allow a direct correlation between AFM heights in TEM-based widths but displayed an AFM-based height of only 1.1 ± 0.2 nm (see Supplementary Figure 18), which itself was too small to be used in the TEM-based studies.

To understand the helical structure of these simulated polymers, the stereogenic nature of the ~N=S(=O)F–O~ linker must be considered. For molecular modeling studies, a 32-mer model of polymer **3–23** was constructed (see Supplementary Table 2 on page 67). This

was achieved by copying repeat units of an enantiomerically pure monomer (in this case the (*R*)-configuration at the stereogenic sulfur center), by first making the dimer, and then doubling four more times to obtain the 32-mer model. The helical structures obtained after geometry optimization correlate well with the experimental observations.

These observations warrant further comment: i) Helicity is not exclusive to homochiral polymer models. Upon changing one or more configurations in the chain comprising 64 chiral sulfur atoms, the helicity is retained. Also, if *S* configuration is built into the model polymer at regular intervals (e.g., $R_7SR_7SR_7SR_7SR_7SR_7S$), the calculated results again predict the formation of a helical polymer, albeit with a slightly different diameter and pitch. However, with a large and fully randomized variation of *R* and *S* configurations, no helicity was predicted by the molecular modeling. The modeling data collectively indicate robustness in the helical shape that corresponds to a thermodynamic minimum (see Supplementary Table 2 on pages 67–72). ii). Optical activity in the polymer product would not be expected in the absence of chiral induction; circular dichroism measurements confirm this sentiment. iii) The observed polymer helicity suggests a degree of self-organization to give the thermodynamically preferred tertiary structures. These structures would inevitably require the SuFEx bond-forming reactions to be reversible to flip the configuration at a given sulfur center. To investigate this notion, we treated the enantiomerically pure model substrate (*R*)-(–)-**16** (>99% ee; the absolute configuration was determined by the crystal structure, see Supplementary Page 39) with DBU in NMP. Significant racemization was observed after 16 h at room temperature (equation 1).[48] However, while racemization does not occur quickly for this particular model substrate, it may indeed for a polymer with an energetic preference for forming a helix.

A reaction mixture comprising **16** (0.07 M in CD_3CN) and DBU (0.1 M) was monitored by ^1H NMR at room temperature, revealing a degree of hydrolysis after 22 hours (see Supplementary page 42). However, the optically pure sulfurimidate (–)-**17** (98% ee) is stable to racemization in both 0.1 M DBU and BEMP (0.1 M) at room temperature in CD_3CN (see Supplementary pages 47–49). The racemization of *R*-(–)-**16** is thought to occur by DBU mediated reversible formation of the S(VI) cation. The polymer **3–1** (0.028 M repeating unit in DMF-d_7) and DBU (0.1 M) was observed by ^1H NMR to undergo significant hydrolysis after 11 hours (see Supplementary page 43), indicating a greater propensity for racemization than the corresponding (*R*)-(–)-**16**.

Finally, the collective spectroscopic techniques engaged (AFM, SEM, AES, TEM) lead us to conclude that the polymers arise without significant branching. This observation is consistent with the established reactivity trend of SOF_4 derivatives[23]. For example, when the monomer **1–1** was reacted to completion with 4 equivalents of the aryl silyl ether **2–13** for 10 min, the ratio of products **18** to **19** was over 100 : 1 (equation 2). The observed chemoselective preference during polymerization explains the preferential formation of the linear (unbranched) polymer.

Conclusions:

In summary, we have described a new class of modular SuFEx copolymers linked through SOF_4 derived [-N=S(=O)(F)–O-] hubs and bisphenol monomers. These polymers were prepared with high efficiency from the corresponding bis(iminosulfur oxydifluorides) and bis(aryl silyl ethers) under DBU catalyzed SuFEx conditions. The multidimensional connectivity of the S(VI) hub derived from SOF_4 presents a unique opportunity for post-polymerization modification, which was demonstrated here through the controlled and near the quantitative installation of aryl silyl ethers and amines to the spine of the polymer. Further derivatization of the alkyne-decorated SuFEx-polymer **7** was demonstrated using CuAAC click chemistry, delivering one new functional polymer **9** with potential application in polymer-drug conjugates. The triphenylvinyl phenoxy-branched polymer **5** showed an aggregation-induced emission (AIE) effect, while the polymer with pendant ferrocenes **15** may exhibit interesting potential properties[49]. Collectively, these examples showcase the potential of SOF_4-derived materials in diverse applications. Detailed structure studies combining AFM, high-resolution SEM, high-resolution TEM, and molecular modeling, reveal helical polymer structures, which correlates well with the NMR data of the polymers. While the mechanism of forming these unique polymers is not yet understood, the helical structures suggest an unprecedented degree of self-referential control, stereochemical, and otherwise, over the constitution of the evolving polymer chains.

Methods

Full details of the methods are provided in the Supplementary Information.

1. General Information:

^{1}H spectra were recorded on Bruker AV-600 and Bruker AV-400 NMR instruments; ^{13}C NMR spectra were recorded on a Bruker AV-600; ^{19}F NMR spectra were recorded on a Bruker AV-400. The chemical shifts (δ) are expressed in parts per million relative to TMS or residual deuterated acetonitrile, DMF, and DMSO as internal standards. Proton magnetic resonance (^{1}H NMR) spectra were recorded at 600 or 400 MHz. Carbon magnetic resonance (^{13}C NMR) spectra were recorded at 151 MHz or 101 MHz. Fluorine magnetic resonance (^{19}F NMR) spectra were recorded at 376 MHz. NMR acquisitions were performed at 295 K unless otherwise noted. Abbreviations are s, singlet; d, doublet; t, triplet; q, quartet, p, pentet; br s, broad singlet. Infrared spectra were recorded as pure, undiluted samples using ThermoNicolet Avatar 370 Fourier transform infrared spectrometer with a Smart MIRacle™ HATR attachment. Melting points (mp) were determined using a Thomas-Hoover melting point apparatus and are uncorrected. GC-MS data were recorded on an Agilent 7890A GC system with an Agilent 5975C Inert MSD system or SHIMADZU GCMS-QP2010 SE operating in the electron impact (EI+) mode. LC-MS was performed on an Agilent 1260 LC/MSD with an Agilent 6120 quadrupole mass spectrometer (electrospray ionization, ES) or a Waters ACQUITY ARC-ACQUITY QDa eluting with 0.1% trifluoroacetic acid in H_2O and 0.05% trifluoroacetic acid in CH_3CN. Waters UPLC (ACQUITY Arc) and Waters preparative HPLC (2545) were used for enantiomeric excess analysis and chiral sample preparation. High-resolution mass spectrometry was performed on an Agilent ES-

TOF instrument. Single crystal X-ray diffraction was tested on an Agilent SuperNova Single Crystal Diffractometer. Precoated Merck F-254 silica gel plates were used for thin layer analytical chromatography (TLC) and visualized with short-wave UV light or by potassium permanganate stain. Column chromatography was performed using EMD (Merck) Silica Gel 60 (40–63 μm). Extra dry solvents over molecular sieves were purchased from Aldrich or Acros Organics, including acetonitrile (CH_3CN), tetrahydrofuran (THF), dimethylformamide (DMF), and *N*-methyl-2-pyrrolidone (NMP). All of the bis(amines) used in this study are commercially available.

The polymer molecular weight (weight-average, M_w^{ps}) and polydispersity (PDI) relative to polystyrene were measured by Waters 1515 Gel Permeation Chromatography (GPC) system. It was equipped with a diode-array, a refractive index detector 2414, and a series of MZ-Gel *SDplus* 500 Å, 10E3 Å, 10E4 Å columns. The system was calibrated with *Easy Vial PS-M* polystyrene standards (*Agilent Technologies,* Mp = 364000, 217900, 113300, 47190, 30230, 13270, 6940, 2780, 1220, 935, 370, 162 g/mol). HPLC grade DMF was used as a mobile phase with 0.05 mol/L of LiBr as additives (*Acros Organics*, 99.999% grade). The elution rate was 0.8 mL/min (column temperature, 40 °C). All samples/standards were tested at 100 μL loadings (1.0 mg/mL).

The thermal gravimetric analysis (TGA) and differential scanning calorimetry (DSC) analysis were carried out at *Lawrence Berkeley National Laboratory* and *Soochow University*. TGA was carried out on TGA- MS Q5000 under nitrogen using aluminum pans (20 °C/min started from 25 °C and ended at 600 °C). The DSC was carried out on TA Q200 with a heat rate of 5 °C/min.

Procedure for the synthesis of the polymer 3–1 (30 mmol scale)—To a round-bottomed flask (250 mL) with a magnetic stir bar was added the bis(iminosulfur oxydifluoride) **1–1** (12.5 g, 30.0 mmol), BPA-TBS **2–1** (13.7 g, 30.0 mmol) and 40 mL of anhydrous NMP. The flask was sealed with a Suba-Seal® Septa, vacuumized with a needle linked with a pump until no bubbles formed in the solution (5–10 min). Then DBU (91.3 mg, 90 μL, 0.60 mmol, d = 1.018 g/mL) was added into the flask via a needle. After stirring at room temperature for 15 min, the solution became a jam, and the stir bar stopped moving. After staying at room temperature for 3.5 h, 50 mL of DMF was added. The flask was shaken to promote the dissolution, and the resulting solution was poured slowly into 600 mL of MeOH with mechanical stirring. The solution was stirred in MeOH for 20 minutes and filtrated. The white solid was washed with MeOH three times (150 mL × 3) and then dried in the vacuum oven (60 °C) for 24 hours to give 18.0 g of the polymer **3–1** (99%). M_w^{ps} = 197 kDa. PDI = 1.8. T_g (DSC) = 150.8 °C. T_d (5% weight loss, TGA) = 261.2 °C. ^{1}H NMR (600 MHz, DMF-d_7) δ 8.05 (d, J = 8.4 Hz, 4H), 7.58 – 7.36 (m, 12H), 1.70 (s, 6H). ^{13}C NMR (151 MHz, DMF) δ 151.90, 149.29, 144.39 (d, J = 2.7 Hz), 139.14, 130.56, 130.11, 125.68 (d, J = 2.8 Hz), 122.26, 43.87, 31.09. ^{19}F NMR (376 MHz, DMF-d_7) δ 50.69.

AFM, SEM, and TEM Experiments

Atomic force microscope (AFM):

Surface Preparation: A Si (111) wafer with a 0.2° miscut angle along <112> was first cut (10 × 10 mm^2), and subsequently cleaned in a sonication bath with acetone, ethanol and then with Milli-Q water (resistivity >18 MΩ cm). The Si wafer was oxidized in oxygen plasma for at least 20 min. after which the substrates were immersed immediately in water and rinsed thoroughly, followed by drying with a stream of argon. Subsequently, the substrates were etched in an argon-saturated 40% aqueous NH_4F solution for 15 min, rinsed by Milli-Q water and finally dried with a stream of argon. After being, etched, the samples were rinsed with argon-saturated water, and finally blown dry with a stream of argon. These samples were then immediately transferred to an inert atmosphere glove box. Next, the surface was placed into a neat dry and pure 1-hexadecyne solution, which was then subsequently heated. The reactions were performed at 80 °C overnight (typically 16 h). Afterwards, the mixture was allowed to cool to room temperature, the coated surface was taken out of the solution, taken out of the glovebox, and immediately extensively rinsed with pentane and CH_2Cl_2. The sample was then sonicated for 5 min in CH_2Cl_2 to remove physisorbed molecules, after which the samples were blown dry with a stream of dry argon. Before depositing the polymer solution onto such hexadecyne-modified Si(111) surfaces, AFM was used to check that is was atomically flat (RMS roughness < 0.1 nm). Methods to determine the helicity of polymer: The AFM morphology and amplitude maps were first flattened in series by a 1^{rst}-order plane fit and by a 2^{nd} order polynomial line by line fit. Subsequently, a 7×7 weak median filter was applied to reduce the level of noise. Fast Fourier Transform was calculated on the raw cross-sectional profiles after a 0-order profile subtraction. Analysis was performed with the SPIP 8.3 software (Image Metrology, Denmark).

Polymer deposition: Then two drops (ca. 10 μl) of a polymer solution (e.g of **3–23**; 0.1 mg/mL in HPLC grade DCM) were gently dropped on such hexadecyne-coated surface, after which the solvent smoothly evaporated at room temperature without enforcing. The imaging was performed in tapping mode in air using either OMCL-AC240 silicon cantilevers (Olympus Corporation, Japan) with a stiffness of 1.54 N/m, or ultra-sharp silicon tips from NanoAndMore GmbH SHR75, with a stiffness of 3 N/m and radius < 1 nm. Images were flattened with a third-order flattening procedure using the MFP3D software. Topography were typically obtained on two different instruments (Asylum MFP-3D AFM and JEOL JSPM-5400 Scanning Probe Microscope) and displayed near-identical features on both.

Scanning electron microscopy/Auger electron spectroscopy (SEM/AES): AES measurements were performed at room temperature with a scanning Auger electron spectroscopy (JEOL Ltd. JAMP-9500F field emission scanning Auger microprobe) system. Samples were prepared by spreading powder particles over a gold-coated surface. AES spectra were acquired with a primary beam of 2 keV. For Auger elemental analysis, an 8 nm probe diameter was used. Elemental mapping was analyzed by AES. Elemental images were acquired with a primary beam of 2 keV. The take-off angle of the instrument was 0°.

Transmission electron microscopy (TEM/SEM): Polymer solutions (0.2 mg/mL in THF): ultrathin carbon Grid (~4 nm thickness, Tedpella ultrathin carbon film on lacey carbon support film, 400 mesh, copper) was pretreated by plasma cleaner for 10 s, then a drop of the diluted sample in THF was deposed on the grid surface for a few seconds, and the excess of the solution was removed by fiber-free paper. After that, this grid was dipped in uranyl acetate solution then the excess of uranyl solution was removed by fiber-free paper. Here in this study, uranyl acetate was used as a negative stain for imaging. TEM grid was mounted in a single tilt sample holder and then introduced in the microscope for imaging. Microscope: TEM analyses were performed using a Titan FEG-300KV. 4 K Ceta camera and GMS software for data acquisition. *SEM (Scanning Electron Microscope):* Same TEM grid was mounted in SEM: field emission scanning electron microscopy (FE-SEM, Quanta FEG450, FEI) using a solid-state back scattering electron detector (VCD).

Molecular Mechanics Studies: Geometry optimization of the polymers was performed using molecular mechanics calculations using the Polymer Consistent Force Field (PCFF) as implemented in the Dassault Systèmes BIOVIA, Materials Studio 6.0, San Diego molecular modeling package. To this aim, first, the polymer structure was drawn in ChemDraw with 32 repeating units. This structure was transferred in Chem3D, optimized using the MMFF94 force field as implemented in that, and the resulting structure saved and converted to the *.mol format, which can be read by Materials Studio. This structure was then imported in Materials Studio and further optimized using the Forcite minimizer and the PCFF force field, with “high-convergence” criteria and the “smart optimizer” algorithm. No further restrictions were applied.

Quantum-chemical calculations: The quantum chemical calculations were run using the Gaussian 16 suite of programs with the functionals, basis sets, and solvent models as implemented in there. We used the xB97XD functional, the SMD solvation model, and standard 6–311+G(d,p) basis sets for our calculations. The keywords used to run these calculations and the obtained zero-point energy-corrected energies are given below in Hartree. This yields the reaction energies given in the most right column (in kcal/mol).

Data availability statement—The authors confirm that the data supporting the findings of this study are available within the article and its supplementary materials.’Crystallographic data for the structures reported in this Article have been deposited at the Cambridge Crystallographic Data Centre, under deposition numbers CCDC 2026570 [*R*-(−)-**16**]. Copies of the data can be obtained free of charge via https://www.ccdc.cam.ac.uk/structures/.

Additional information—Supplementary information is available in the online version of the paper. Reprints and permissions information is available online at www.nature.com/reprints. Publisher’s note: Springer Nature remains neutral with regard to jurisdictional claims in published maps and institutional affiliations. Correspondence and requests for materials should be addressed to K. B. S.

Supplementary Material

Refer to Web version on PubMed Central for supplementary material.

Acknowledgments

The authors gratefully acknowledge financial support from the National Science Foundation (CHE-1610987 to KBS) and the NIH (R01GM093282 to PW), the ARC for supporting Future Fellowship FT170100156 (JEM). Guangdong Natural Science Funds for Distinguished Young Scholar (2018B030306018), the Program for Guangdong Introducing Innovative and Entrepreneurial Teams (2017ZT07C069), and the Pearl River Talent Recruitment Program (2019QN01L111) to SL. National Science Foundation of China (#21871208 to HZ, 21971260 to SL) and King Abdulaziz University (to HD and HZ). Part of the work was carried out as a user project at the Molecular Foundry, supported by the Office of Science, Office of Basic Energy Sciences, of the US Department of Energy under Contract No. DE-AC02-05CH11231. The authors thank Dr. Linfeng Liang (Shanxi University) for assistance with X-ray single-crystal structural analyses and Dr. Simone Ruggeri and Barend van Lagen (Wageningen University) for detailed AFM analysis. The authors are grateful to Dr. John R. Cappiello for proofreading and advice on the manuscript.

Abbreviations:

BEMP	2-*tert*-butylimino-2-diethylamino-1,3-dimethyl perhydro-1,3,2-diazaphosphorine
DBU	1,8-diazabicyclo[5.4.0]undec-7-ene
TMS	trimethylsilyl
TBS	*tert*-butyldimethylsilyl

References:

1. Sharpless KB & Kolb HC Book of Abstracts, 217th ACS National Meeting, Anaheim, CA, March 21–25, ORGA-105, Accession Number 1999:145538, (1999).
2. Kolb HC, Finn MG & Sharpless KB Click chemistry: Diverse chemical function from a few good reactions. Angew. Chem. Int. Ed. 40, 2004–2021, (2001).
3. Tornoe CW, Christensen C & Meldal M Peptidotriazoles on solid phase: 1,2,3 -triazoles by regiospecific copper(I)-catalyzed 1,3-dipolar cycloadditions of terminal alkynes to azides. J. Org. Chem. 67, 3057–3064, (2002). [PubMed: 11975567]
4. Rostovtsev VV, Green LG, Fokin VV & Sharpless KB A stepwise Huisgen cycloaddition process: Copper(I)-catalyzed regioselective “ligation” of azides and terminal alkynes. Angew. Chem. Int. Ed. 41, 2596–2599, (2002).
5. Dong J, Krasnova L, Finn MG & Sharpless KB Sulfur(VI) Fluoride Exchange (SuFEx): Another Good Reaction for Click Chemistry. Angew. Chem. Int. Ed. 53, 9430–9448, (2014).
6. Kolb HC & Sharpless KB The growing impact of click chemistry on drug discovery. Drug Discov. Today 8, 1128–1137, (2003). [PubMed: 14678739]
7. Moses JE & Moorhouse AD The growing applications of click chemistry. Chem. Soc. Rev. 36, 1249–1262, (2007). [PubMed: 17619685]
8. Moorhouse AD & Moses JE Click chemistry and medicinal chemistry: A case of “Cyclo-Addiction.” Chemmedchem 3, 715–723, (2008). [PubMed: 18214878]
9. Thirumurugan P, Matosiuk D & Jozwiak K Click Chemistry for Drug Development and Diverse Chemical-Biology Applications. Chem. Rev. 113, 4905–4979, (2013). [PubMed: 23531040]
10. Rouhanifard SH, Nordstrom LU, Zheng T & Wu P Chemical probing of glycans in cells and organisms. Chem. Soc. Rev. 42, 4284–4296, (2013). [PubMed: 23257905]
11. McKay CS & Finn MG Click Chemistry in Complex Mixtures: Bioorthogonal Bioconjugation. Chem. Biol. 21, 1075–1101, (2014). [PubMed: 25237856]

12. Xi W, Scott TF, Kloxin CJ & Bowman CN Click Chemistry in Materials Science. Adv. Funct. Mater. 24, 2572–2590, (2014).
13. Liu Y et al. Click chemistry in materials synthesis. III. Metal-adhesive polymers from Cu(I)-catalyzed azide-alkyne cycloaddition. J. Polym. Sci. A Polym. Chem. 45, 5182–5189, (2007).
14. Diaz DD et al. Click chemistry in materials synthesis. 1. Adhesive polymers from copper-catalyzed azide-alkyne cycloaddition. J. Polym. Sci. A Polym. Chem. 42, 4392–4403, (2004).
15. Wu P et al. Efficiency and fidelity in a click-chemistry route to triazole dendrimers by the copper(I)-catalyzed ligation of azides and alkynes. Angew. Chem. Int. Ed. 43, 3928–3932, (2004).
16. van Steenis DJVC, David ORP, van Strijdonck GPF, van Maarseveen JH & Reek JNH Click-chemistry as an efficient synthetic tool for the preparation of novel conjugated polymers. Chem. Commun, 4333–4335, (2005).
17. Srinivasachari S, Liu Y, Zhang G, Prevette L & Reineke TM Trehalose Click Polymers Inhibit Nanoparticle Aggregation and Promote pDNA Delivery in Serum. J. Am. Chem. Soc. 128, 8176–8184, (2006). [PubMed: 16787082]
18. Gahtory D et al. Quantitative and Orthogonal Formation and Reactivity of SuFEx Platforms. Chem. Eur. J. 24, 10550–10556, (2018). [PubMed: 29949211]
19. Randall JD et al. Modification of Carbon Fibre Surfaces by Sulfur-Fluoride Exchange Click Chemistry. Chemphyschem 19, 3176–3181, (2018).
20. Kassick AJ et al. SuFEx-based strategies for the preparation of functional particles and cation exchange resins. Chem. Commun. 55, 3891–3894, (2019).
21. Fan H et al. Sulfur (VI) Fluoride Exchange Polymerization for Large Conjugate Chromophores and Functional Main-Chain Polysulfates with Nonvolatile Memory Performance. Chempluschem 83, 407–413, (2018). [PubMed: 31957370]
22. Park S et al. SuFEx in Metal-Organic Frameworks: Versatile Postsynthetic Modification Tool. ACS Appl. Mater. Interfaces 10, 33785–33789, (2018). [PubMed: 30230813]
23. Li S, Wu P, Moses JE & Sharpless KB Multidimensional SuFEx Click Chemistry: Sequential Sulfur(VI) Fluoride Exchange Connections of Diverse Modules Launched From An SOF_4 Hub. Angew. Chem. Int. Ed. 56, 2903–2908, (2017).
24. Gao B, Li S, Wu P, Moses JE & Sharpless KB SuFEx Chemistry of Thionyl Tetrafluoride (SOF_4) with Organolithium Nucleophiles: Synthesis of Sulfonimidoyl Fluorides, Sulfoximines, Sulfonimidamides, and Sulfonimidates. Angew. Chem. Int. Ed. 57, 1939–1943, (2018).
25. Zheng Q, Dong J & Sharpless KB Ethenesulfonyl Fluoride (ESF): An On-Water Procedure for the Kilogram-Scale Preparation. J. Org. Chem. 81, 11360–11362, (2016). [PubMed: 27764941]
26. Smedley CJ et al. 1-Bromoethene-1-sulfonyl fluoride (BESF) is another good connective hub for SuFEx click chemistry. Chem. Commun. 54, 6020–6023, (2018).
27. Leng J & Qin H-L 1-Bromoethene-1-sulfonyl fluoride (1-Br-ESF), a new SuFEx clickable reagent, and its application for regioselective construction of 5-sulfonylfluoro isoxazoles. Chem. Commun. 54, 4477–4480, (2018).
28. Thomas J & Fokin VV Regioselective Synthesis of Fluorosulfonyl 1,2,3-Triazoles from Bromovinylsulfonyl Fluoride. Org. Lett. 20, 3749–3752, (2018). [PubMed: 29906123]
29. Dong J, Sharpless KB, Kwisnek L, Oakdale JS & Fokin VV SuFEx-Based Synthesis of Polysulfates. Angew. Chem. Int. Ed. 53, 9466–9470, (2014).
30. Gao B et al. Bifluoride-catalysed sulfur(VI) fluoride exchange reaction for the synthesis of polysulfates and polysulfonates. Nat. Chem. 9, 1083–1088, (2017). [PubMed: 29064495]
31. Wang H et al. SuFEx-Based Polysulfonate Formation from Ethenesulfonyl Fluoride-Amine Adducts. Angew. Chem. Int. Ed. 56, 11203–11208, (2017).
32. For reactions performed on a 5 mmol scale, a slight increase in catalyst loading of 3 mol% of DBU was required for efficient polymerization.
33. Cowie JMG & Arrighi V Polymers: Chemistry and Physics of Modern Materials. 3rd edn, 29–56 (CRC Press, 2007).
34. Gauthier MA, Gibson MI & Klok H-A Synthesis of Functional Polymers by Post-Polymerization Modification. Angew. Chem. Int. Ed. 48, 48–58, (2009).

35. Boaen NK & Hillmyer MA Post-polymerization functionalization of polyolefins. Chem. Soc. Rev. 34, 267–275, (2005). [PubMed: 15726162]
36. Yatvin J, Brooks K & Locklin J SuFEx on the Surface: A Flexible Platform for Postpolymerization Modification of Polymer Brushes. Angew. Chem. Int. Ed. 54, 13370–13373, (2015).
37. Oakdale JS, Kwisnek L & Fokin VV Selective and Orthogonal Post-Polymerization Modification using Sulfur(VI) Fluoride Exchange (SuFEx) and Copper-Catalyzed Azide-Alkyne Cycloaddition (CuAAC) Reactions. Macromolecules 49, 4473–4479, (2016).
38. Brooks K et al. SuFEx Postpolymerization Modification Kinetics and Reactivity in Polymer Brushes. Macromolecules 51, 297–305, (2018).
39. Hong Y, Lam JWY & Tang BZ Aggregation-induced emission. Chem. Soc. Rev. 40, 5361–5388, (2011). [PubMed: 21799992]
40. The observed ratio would yield 93%, but it was noted that the one proton in terminal alkynes sometimes showed as slightly less than 1.00 in ^{1}H NMR.
41. del Amo DS et al. Biocompatible Copper(I) Catalysts for in Vivo Imaging of Glycans. J. Am. Chem. Soc. 132, 16893–16899, (2010). [PubMed: 21062072]
42. Wang W et al. Sulfated Ligands for the Copper(I)-Catalyzed Azide-Alkyne Cycloaddition. Chem. Asian J. 6, 2796–2802, (2011). [PubMed: 21905231]
43. Yashima E, Maeda K, Iida H, Furusho Y & Nagai K Helical Polymers: Synthesis, Structures, and Functions. Chem. Rev. 109, 6102–6211, (2009). [PubMed: 19905011]
44. Nakano T & Okamoto Y Synthetic helical polymers: Conformation and function. Chem. Rev. 101, 4013–4038, (2001). [PubMed: 11740925]
45. Dassault Systems BIOVIA, Materials Studio 6.0, San Diego.
46. Li Y et al. Hybrids of Organic Molecules and Flat, Oxide-Free Silicon: High-Density Monolayers, Electronic Properties, and Functionalization. Langmuir 28, 9920–9929, (2012). [PubMed: 22587009]
47. Bose K, Lech CJ, Heddi B & Anh Tuan P High-resolution AFM structure of DNA G-wires in aqueous solution. Nat. Commun. 9, 1959, (2018). [PubMed: 29773796]
48. Liang D-D et al. Silicon-Free SuFEx Reactions of Sulfonimidoyl Fluorides: Scope, Enantioselectivity, and Mechanism, Angew. Chem. Int. Ed. 59, 7494–7500, (2020).
49. Pietschnig R Polymers with pendant ferrocenes, Chem. Soc. Rev. 45, 5216–5231, (2016). [PubMed: 27156979]

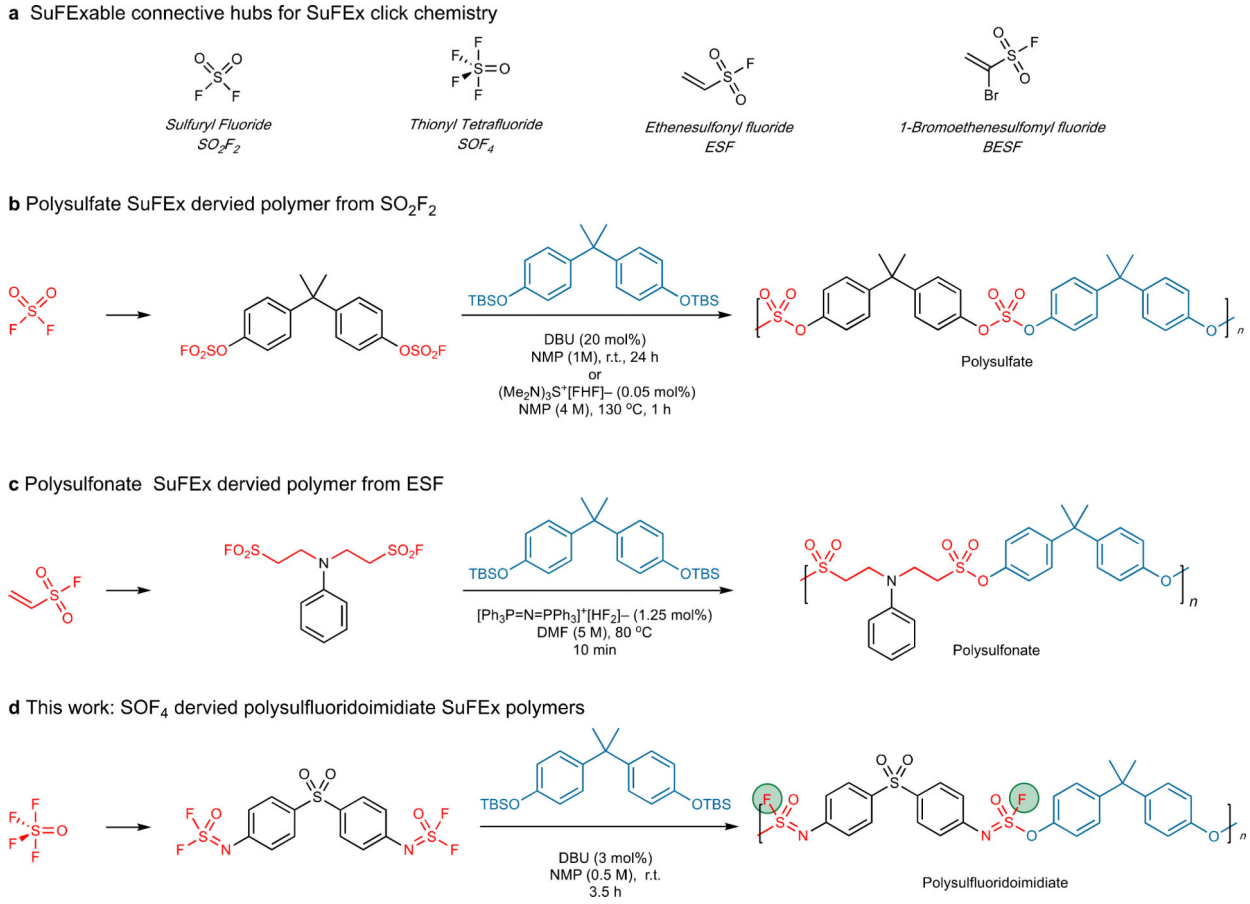

Figure 1:

SuFEx click chemistry for polymer synthesis a. Connective SuFEx hubs for creating S-centered linkages; b. Polysulfate materials derived from SO_2F_2; c. Polysulfonate materials obtained from ESF. d. New polysulfluorido-imidate materials derived from the multidimensional SuFEx connector SOF_4. Connective hubs are shown in red; bisphenol monomers are shown in pale blue; SuFExable S–F bonds for post-polymerization backbone modification are shown in green.

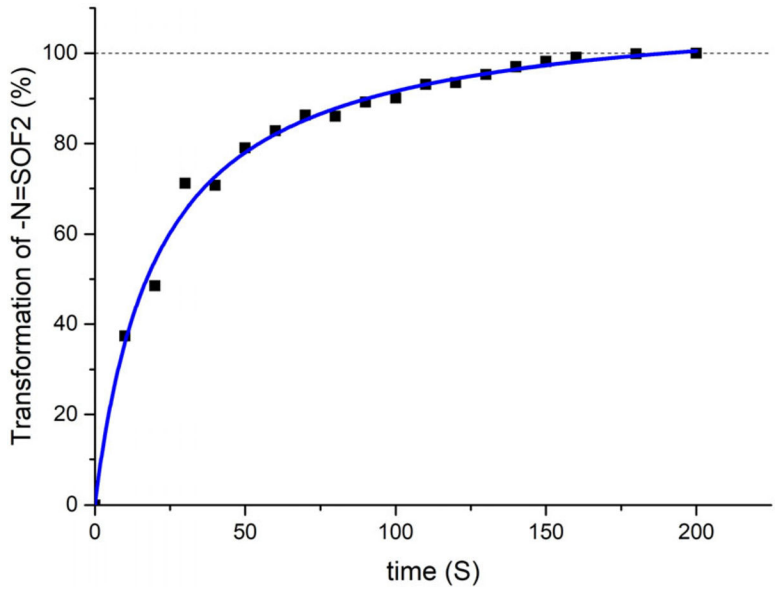

Figure 2.

Kinetic profile of the polymerization of **1–1**(1 mmol**)** and **2–1**(1 mmol); 0.5 M in NMP, 3 mol% DBU. The monomer conversion was completed within 200 seconds, indicates a very fast reaction. The transformation data are calculated based on the ratio of ^{19}F signal integral of the remaining -N=SOF_2 at the indicated time compared to the integral of -N=SOF_2 before adding DBU with ^{19}F NMR (no solvent mode).

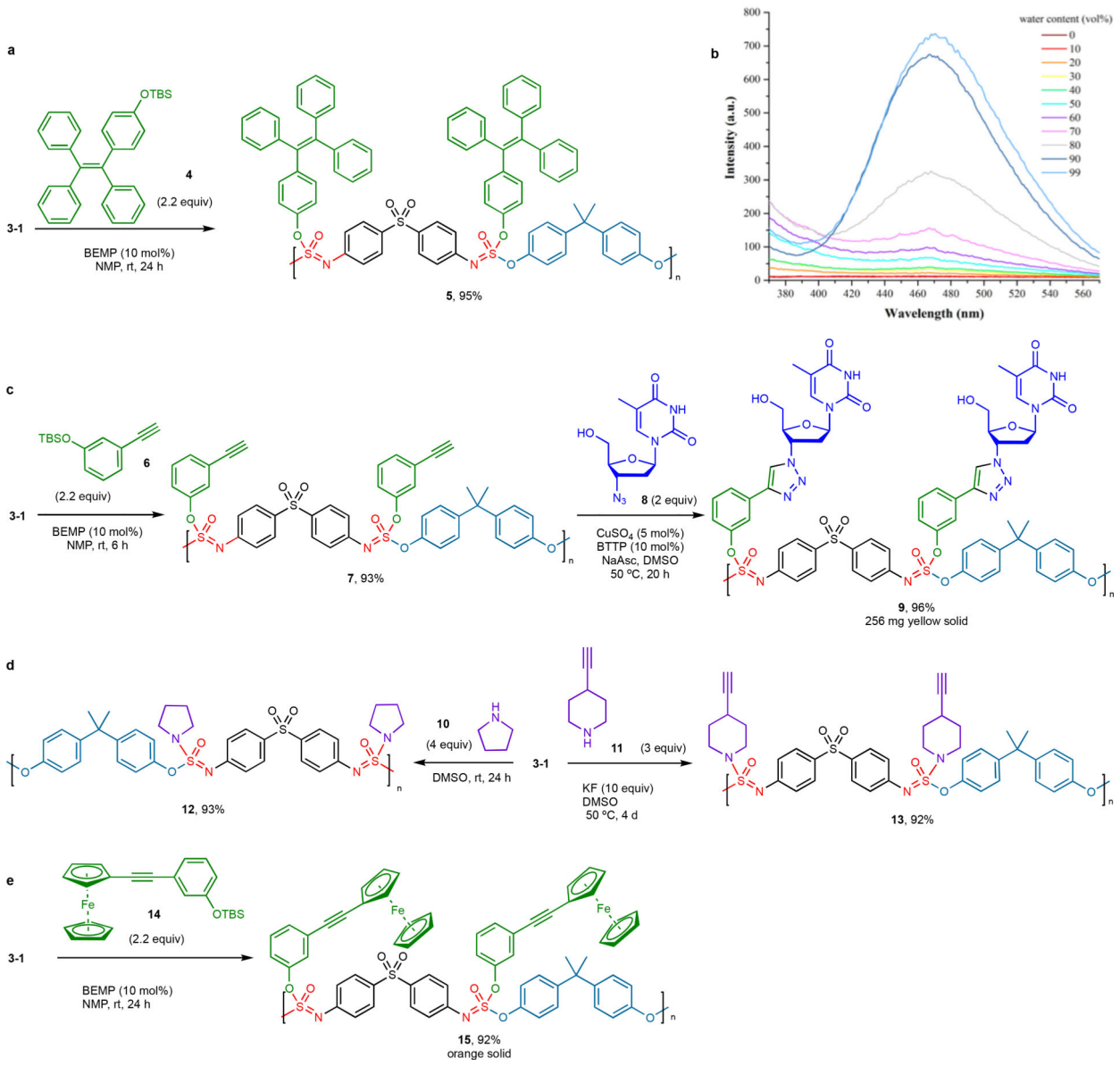

Figure 3.

Post-polymerization modification of polymer **3–1** using sequential SuFEx and CuAAC click chemistry: a. SuFEx Synthesis of triphenylvinyl phenoxy-branched polymer **5**; b. Fluorescence spectra of **5** (5 μM of the repeat unit) in THF/H_2O (v/v = 100:0 ~ 1:99) indicates a strong AIE effect; c. Stepwise synthesis of alkyne-functionalized polymer **7** by SuFEx (new moiety is shown in green), and subsequent CuAAC synthesis of polymer **9** with an azide-bearing AZT derivative (shown in dark blue); d. Post-polymerization SuFEx modification of **3–1** with secondary amines (shown in purple); e. Introduction of ferrocene unit (shown in green) to the polymer chain. All the yields are the weight of polymer recovery compared with the 100% substituted polymer's theoretical weight.

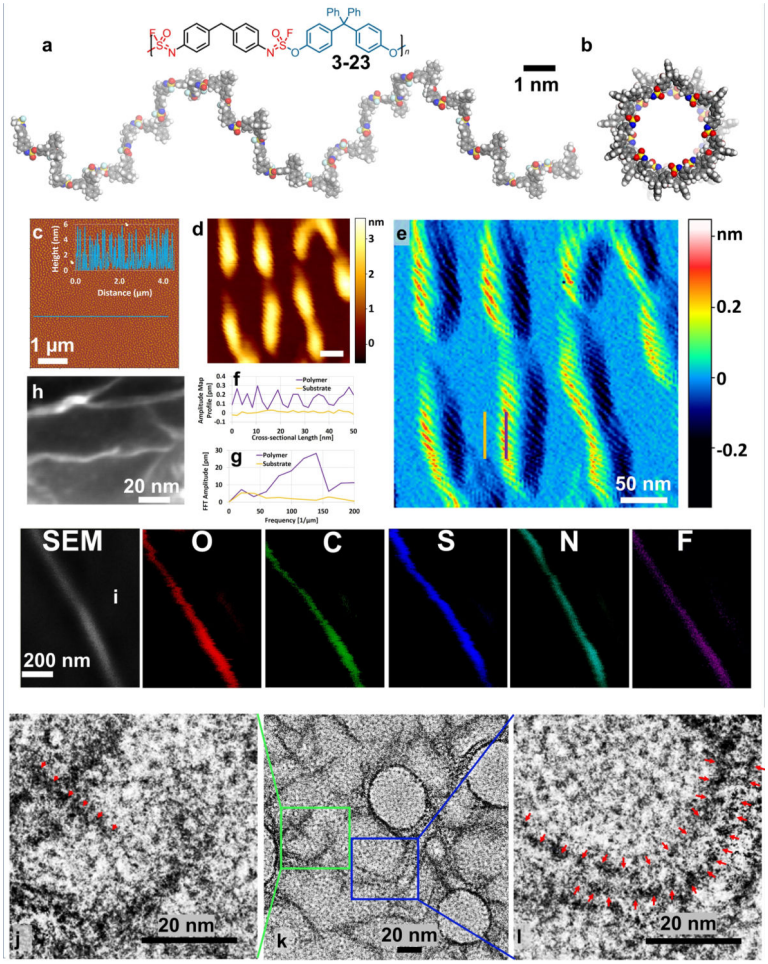

Figure 4.

(a-b) PCFF-optimized structure of **3–23** (side view and top view) Color code of atoms: C, grey; O, red; N, blue; F, cyan; S, yellow; and H, white. (c) AFM height image (5 × 5 μm^2 with the topographic height profile as inset). Analysis of the structural organization and periodicity of the helical polymer: (d) 3-D topographic (scale bar 50 nm) and (e) amplitude map of polymer **3–23** on hexadecyne-coated Si(111) surfaces, with cross sections over a polymer chain (vertical purple line) and in parallel over the substrate (vertical yellow line). (f) cross-sectional amplitude profiles acquired on the polymer (purple) and the substrate (yellow). (g) Fast Fourier Transform of the cross-sectional amplitude profiles on the polymer (purple) and on the substrate (yellow) to extract the dominant frequencies in the signal. (h) High-resolution SEM image of **3–23** deposited on a TEM grid. (i) SEM/AES image of polymer **3–23** coated on hexadecanethiol-modified gold surfaces and AES images on the same surface for the elements O, C, S, N, and F. High-resolution TEM (j–l) images of polymer **3–23** (red marks added as a guide to the eye used to determine pitch).

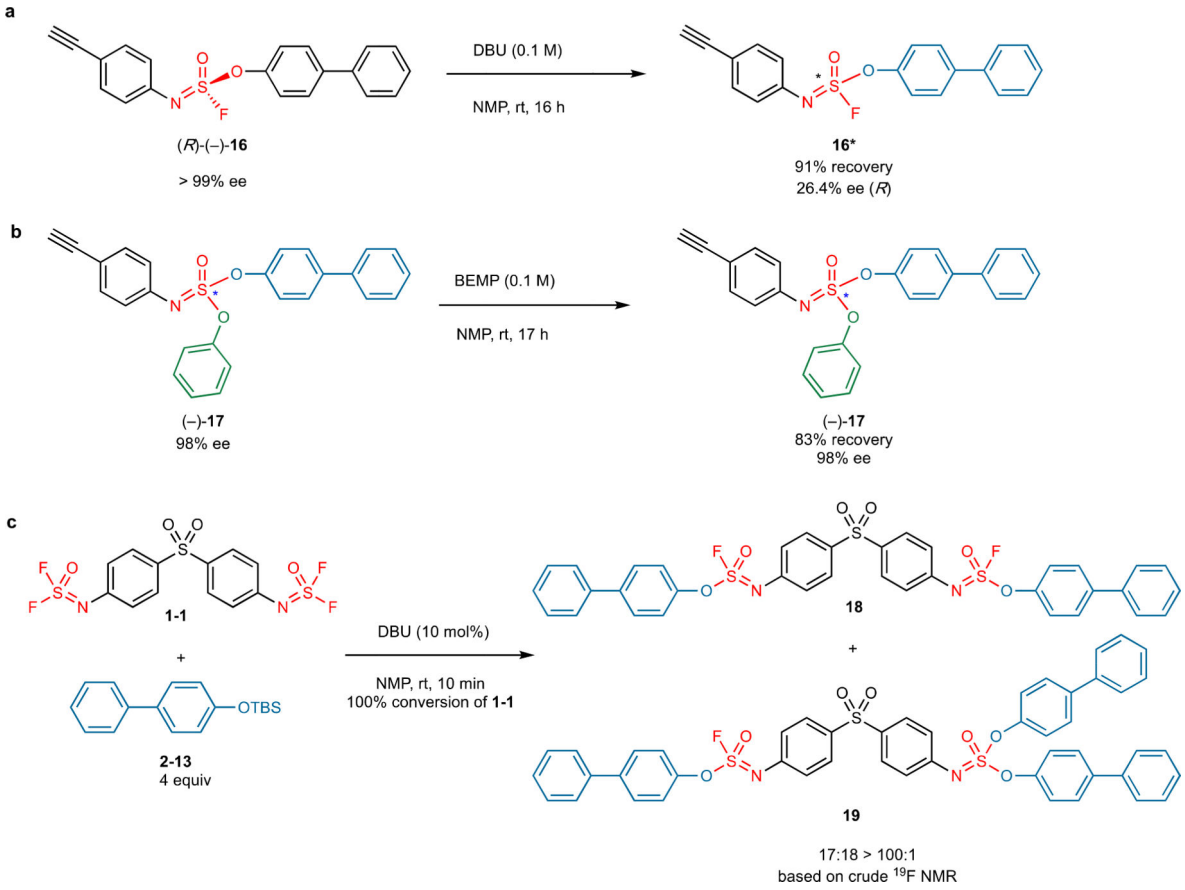

Figure 5.

Racemization experiments of sulfurofluoridoimidate and sulfurimidate in the presence of DBU or BEMP, and reactive selectivity of iminosulfur oxydifluoride with aryl silyl ether. (a) Significant racemization of (*R*)-(–)-**16** appeared after 16 hours in the presence of DBU (0.1 M, NMP). (b) No obvious racemization of (–)-**17** was detected after 17 hours in the presence of BEMP (0.1 M, NMP). (c) The selectivity between the first and the secondary fluoride of iminosulfur oxydifluoride **1–1** is over 100 > 1 even in a large excess of an aryl silyl ether.

Table 1.

Synthesis of SOF_4-derived copolymers by the DBU catalyzed SuFEx polymerization of the bis(iminosulfur oxydifluoride) and bis(silyl ether) monomers.

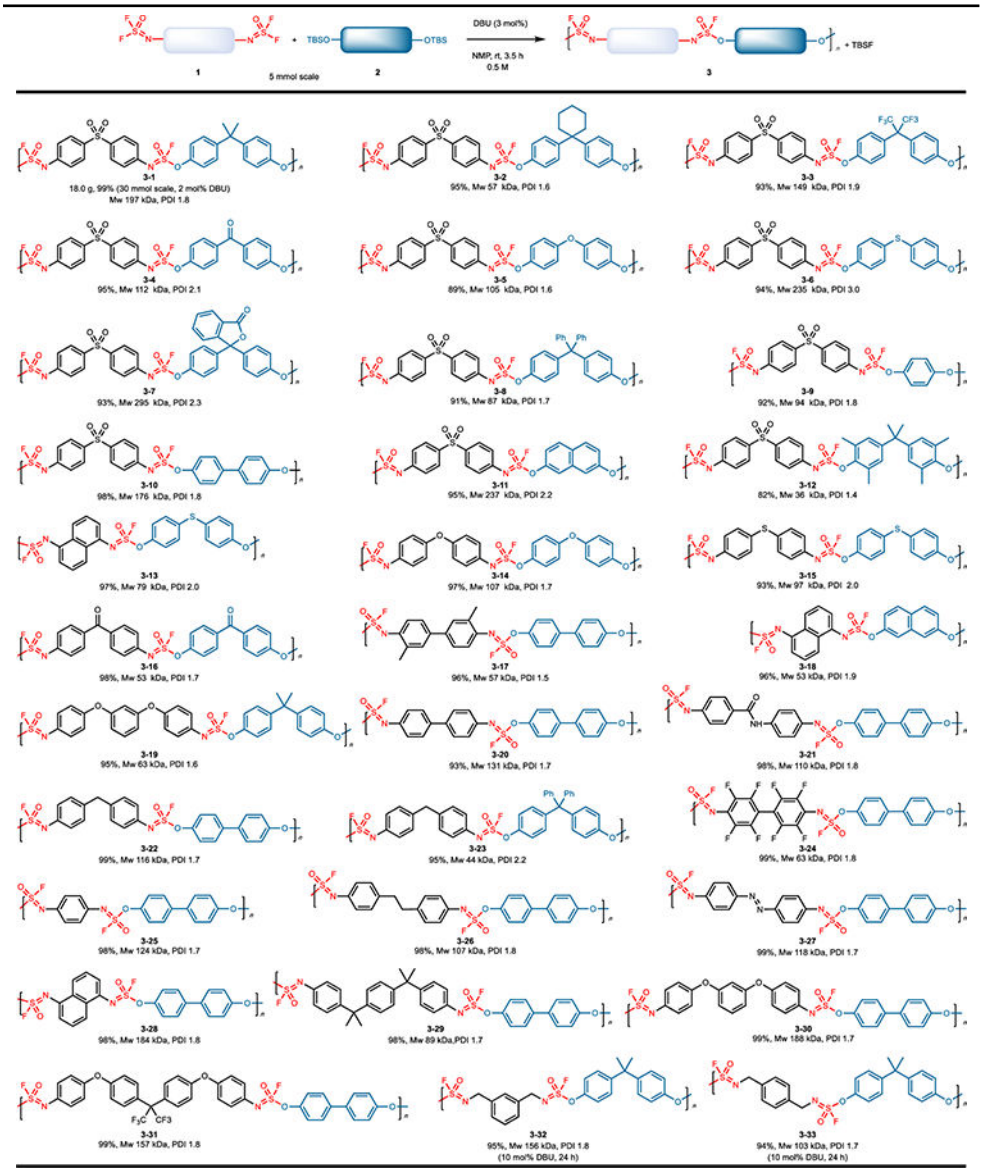

Reaction conditions: For **3–1**: bis(iminosulfur oxydifluoride) (12.49 g, 30 mmol), bisphenol A *tert*-butyldimethylsilyl ether (BPA-TBS) (13.70 g, 30 mmol) and DBU (91.3 mg, 0.6 mmol), were reacted in 40 mL NMP (3.5 h; r.t.). For **3–32**, **3–33**: bis(iminosulfur oxydifluoride) (5 mmol) and bis(silyl ether) (5 mmol) and DBU (0.50 mmol) were reacted in 10 mL NMP (24 h; rt). For others: bis(iminosulfur oxydifluoride) (5 mmol) and bis(silyl ether) (5 mmol) and DBU (0.15 mmol) were reacted in 10 mL NMP (3.5 h; rt).